Forest Ecology and Management 572 (2024) 122317

Contents lists available at ScienceDirect

Forest Ecology and Management

journal homepage: www.elsevier.com/locate/foreco

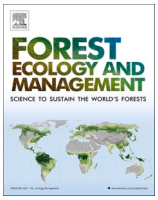

Assessing the recovery of *Pinus canariensis* stands after wildfires and volcanic eruption on La Palma, Canary Islands

Christopher Shatto [a,*], Marvin Kiene [b], Peter Hofmann [c], Anna Walentowitz [a,d], Vincent Wilkens [a], Tobias Heuser [e], Frank Weiser [a,d]

[a] Department of Biogeography, University of Bayreuth, Universitätsstraße 30, Bayreuth 95447, Germany
[b] Department of Animal Ecology I, University of Bayreuth, Universitätsstraße 30, Bayreuth 95447, Germany
[c] Department of Computer Sciences, Deggendorf Institute of Technology, Dieter-Görlitz-Platz 1, Deggendorf 94469, Germany
[d] Bayreuth Center for Ecology and Environmental Science BayCEER, Bayreuth 95440, Germany
[e] Urban Mobility Innovations GmbH, Blütenstraße 15, München, Germany

ARTICLE INFO

Keywords:
NDVI
Pine forest
Tajogaite volcanic eruption
Sulfur
Recovery rate, Theil-Sen

ABSTRACT

The exposure of insular species to local disturbances can influence their evolutionary trajectory resulting in specific adaptations. On the island La Palma, Canary Islands, the archipelago-endemic tree species *Pinus canariensis* forms forest ecosystems and has been described to be adapted to wildfires. The frequency of these in the recent past, however, is higher due to anthropogenic activities. Recent studies suggest that the species traits might also be an evolutionary response to volcanic outbreaks, consisting of massive sulfur dioxide (SO_2) emissions and ash fall. Several stands of *P. canariensis* have been exposed to both disturbances, wildfires and volcanic outbreaks, in the recent past. We assess the recovery of *P. canariensis* after double exposure to these disturbances. *P. canariensis* recovery was assessed based on Sentintel-2 NDVI images within a 7 km radius of the craters of the Tajogaite volcano that erupted in 2021. Within the same area, wildfires occurred in 2009, 2012 and 2016. We used a Generalized Additive Model (GAM) to assess the recovery of *P. canariensis* after volcanic and wildfire disturbances. The model shows the *P. canariensis* forest recovers after the volcanic outbreak with a peak at a distance of 1000–1200 m to the eruption crater, which is in line with our first hypothesis. Our second hypothesis was met with unexpected results, forests exposed to the recent wildfire in 2016 showed an increased recovery, which underlines that *P. canariensis* exhibits traits related to fire adaptation or might also be the result of stand-specific characteristics such as forest height or local topography. The double pressure of volcanic and forest fire disturbances did not lead to suppressed recovery of the Canary-endemic tree species and highlights the resilience of *P. canariensis*.

1. Introduction

Volcanic eruptions are primordial drivers of evolution, particularly on oceanic islands (Nogales et al., 2022). During the volcanically active phase of oceanic islands, eruption events form a pulsed disturbance regime. Eruption occurrence and subsequent impacts vary in magnitude, duration, and intensity, ranging from resetting local assembly processes to widespread destruction of ecosystems (Del Moral & Grishin, 1999; Turner et al., 2020). The physical and geochemical processes of volcanism shape ecosystems, generating heterogeneous landscapes and steep environmental gradients conducive to adaptation and speciation (Doebeli and Dieckmann, 2003; López de Heredia et al., 2014). Volcanism impacts vegetation structures via burial by lava flows and tephra fallout (Mack, 1981; Zobel and Antos, 1997; Kent et al., 2001; Rodríguez Martín et al., 2013), exposure to extreme temperatures, and chemical toxicity from volcanic gases (Clarkson and Clarkson, 1994; Weiser et al., 2022; 2023). Beginning with the eruptions of Krakayau (Ernst & Seward, 1908) and Katmai (Griggs, 1915), research on ecological responses to volcanism has until now focused primarily on tephra burial (Zobel and Antos, 1997; 2022), community succession (Tsuyuzaki, (1991); del

* Corresponding author.
E-mail addresses: christopher.shatto@uni-bayreuth.de (C. Shatto), marvin.kiene@uni-bayreuth.de (M. Kiene), peter.hofmann@th-deg.de (P. Hofmann), anna.walentowitz@uni-bayreuth.de (A. Walentowitz), vincent.wilkens@uni-bayreuth.de (V. Wilkens), tobias.heuser@umi.city (T. Heuser), frank.weiser@uni-bayreuth.de (F. Weiser).

https://doi.org/10.1016/j.foreco.2024.122317
Received 25 September 2024; Accepted 27 September 2024
Available online 11 October 2024

Moral, (2000); Chang et al., (2019); Ishaq et al., (2020); Sáenz-Ceja et al., (2022); Wilkens et al., (in review), biodiversity loss (Nogales et al., 2022), and overall damage to vegetation (Veblen et al., 1977; Tortini et al., 2017; Weiser et al., 2022). While studies have been done on vegetation recovery following volcanic eruptions at Mt. St, Helens in Washington, USA and Mt. Takumbe in Japan (del Moral & Grishin, 1999; del Moral 2000; del Moral & Wood, 2012; Cook & Halpern 2018), until now, research on vegetation recovery following overlapping, interacting volcanic and fire disturbances is still missing.

Island endemics of otherwise commonly herbaceous taxa have been theorized to develop insular woodiness to re-emerge from ash and tephra deposits (Beierkuhnlein et al., 2023). However, surrounding tree species have long been exposed to extreme temperatures and volcanic gases like sulfur dioxide (SO_2) during eruptions as they are only partially buried by pyroclastic flows. This has given rise to the highly resilient tree species *Pinus canariensis* C. Sm which has formed near monodominant stands across the western Canary Islands (López de Heredia et al., 2010; Nogales et al., 2022), thus the terms *P. canariensis* forest and Canary Pine forest are used here interchangeably. *P. canariensis* is well-known as a highly fire-adapted species due to its thick bark, its prowess as a colonizer of bare soils, serotinous cones forming the canopy seed bank, and near immediate resprouting following severe burning (Climent et al., 2004; Pausas & Keeley, 2017). However, these adaptations to fire could just be a side-effect of species adaptations to volcanism (Nogales et al., 2022). That is, historically, forest fires have rarely occurred more than once every 20 years on the islands (Arévalo et al., 2001). Before the appearance of humans, microcharcoal as an indicator of wildfires was very rare, hinting at even fewer fire events (De Nascimento et al., 2009; Nogué et al., 2013). Since the 1960s, La Palma has seen a shift in fire frequency as land use changes have led to the proliferation of large-scale, nonfrequent burns opposed to small-scale, frequent ones (Molina-Terrén et al., 2016). Nonetheless, the resilient traits of *P. canariensis* have mainly been researched following fire (Page, 1974; Arévalo et al., 2001; Climent et al., 2002; 2004,; Fernandes et al., 2008; Keeley, 2012; Méndez et al., 2015; Molina-Terrén et al., 2016; Chano et al., 2023). In this study, we monitor the recovery of *P. canariensis* for the first time after a volcanic eruption and recent wildfires.

In 2021, the Tajogaite volcano erupted on the island of La Palma, Canary Islands, Spain, serving as the island's largest and longest (19 September – 13 December 2021) volcanic eruption within the historical record (Longpré and Felpeto, 2021). The lava stream flowed down the western slope of the Cumbre Vieja ridge, covering nearly 1241 ha (CEMS, n.d.). The lava engulfed immense swaths of land, destroying urban areas, roads, as well as cultural landscapes and natural vegetation. Ash blanketed the island, depositing over 23 million m^3 of material over 65 km^2 (Bonadonna et al., 2022; Shatto et al., 2024), releasing even more into the atmosphere. Despite the pine forest around the new crater being partially buried in ash up to nearly 7 m deep (Shatto et al., 2024), unburied pine stands experienced intense SO_2 exposure at over 1 Tg SO_2 emitted during the eruption (IGME, 2022), leading to widespread chlorosis and defoliation of needles within a 7 km radius of the volcano (Fig. 1; Weiser et al., 2022).

The Tajogaite eruption provides an opportunity to examine pine forest resilience to the various impacts related to volcanism besides lava flows. Additionally, effects of interactions between different types of disturbances become apparent. Previous impacts such as wildfires can modify stand dynamics after volcanic eruptions (Burton et al., 2020). The temporal dimensions of disturbance effects extend beyond that of just their initial abruptness (e.g., magnitude, severity) and the related loss of biomass (Pickett and White, 1985). The pulsed nature of disturbances reflects physical impacts combined with modulations of resource flows (Yang and Naeem, 2008). However, linkages between abiotic impacts and biotic responses are often difficult to identify a posteriori. This results from non-synchronized time scales such as lagged responses, and complex interactions between biotic and abiotic compartments

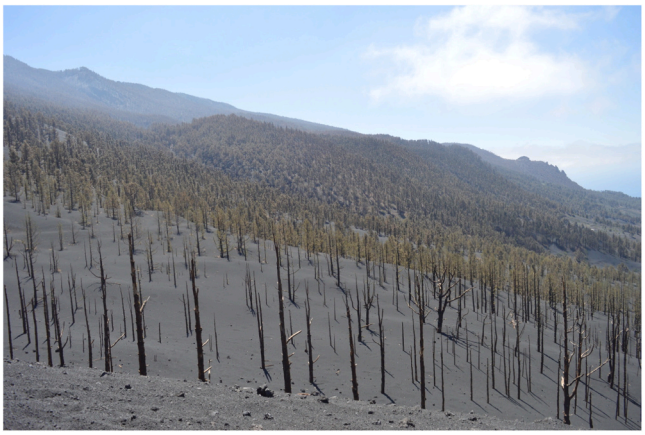

Fig. 1. *P. canariensis* forest near the Tajogaite volcano showing damage gradient of complete defoliation of needles in the foreground and severe chlorotic damage in the distance. Photo taken by Anna Walentowitz.

(Ogle et al., 2015; Buma 2015). For example, forest fires impact ecosystems by altering nutrient cycles, with immediate increases in soil nitrogen that diminish over two decades and initial decreases in phosphorus that eventually stabilize (Durán et al., 2008; 2009,). Additionally, highly frequent fires may reduce the intensity of future fires but can increase soil erosion on steep slopes (Harvey et al., 2016; Mora et al., 2016), eradicating many benefits of fire to the ecosystem. Investigating how ecological patterns and processes respond to perturbations at various time scales is crucial for understanding ecosystem dynamics and predicting ecosystem response to future environmental changes (Johnstone et al., 2016; Burton et al., 2020). Research on disturbance interactions is imperative, as compound disturbances can cause rapid and significant alterations to ecosystems (Turner et al., 2020).

We aim to assess the recovery of *P. canariensis* stands on La Palma after double exposure to disturbances, namely wildfires and volcanic eruption (i.e., exposure to SO_2). Weiser et al. (2022) found distance to be the strongest driver of vegetation damage related to SO_2 emissions by the Tajogaite volcano. Therefore, we first hypothesize that recovery rate will follow hump-shaped curved with distance. Pine stands close to the crater will show little to no recovery due to the intense SO_2 damage and subsequent mortality. Pine stands at intermediate distances will exhibit the highest recovery rates due to their exceptional resilience and the severity of damage causing a high difference in greenness compared to healthy conditions. Pine stands located far away from the crater will not show a high recovery rate due to the comparatively mild damage and the resulting small difference in greenness.

As multiple fires have impacted La Palma in recent years, we also assess the recovery rate of pine stands burned at different times to see if recent fire history affects pine stand response to SO_2 exposure. Canary Pine forests recover quickly from fire but may still take several years to a decade to fully recover (Climent et al., 2004; Méndez et al., 2015). In this case, the lingering effects of the 2016 fire overlap with the eruption and subsequent SO_2 emissions, forming a compound disturbance (Paine et al., 1998; Buma and Wessman, 2011). We secondly hypothesize that stands burned by the most recent fire in 2016 will be slower to recover than stands that had burned earlier or not at all as there was too little time between disturbances for pine stands to recover fully.

2. Materials and methods

2.1. Study area

This study focuses on the island of La Palma, Canary Islands, Spain (28°26′ to 28°51′N and 18°00′ to 17°43′W). La Palma is the most northwestern island of the Canary archipelago and is located ca. 420 km

off the west coast of North Africa. The complex topography of the island, which reaches an altitude of 2426 m a.s.l. as well as its positioning along trade wind corridors results in variable temperature and precipitation regimes across the island (Garzón-Marchado et al., 2012).

Pine forests represent the most extensive ecosystem, covering approximately 248 km^2 of the island (approximately 35 % of the surface area) and ranging from 300 – 400 m to roughly 2200 m a.s.l. In contrast to other islands of the archipelago, they exhibit natural dynamics. Plantations are rare.

2.2. Remote sensing and data retrieval

Sentinel-2 imagery was selected to investigate pine forest change due to SO_2 exposure. The Sentinel-2 constellation is particularly well suited for time series analysis given the spatial resolution (10 m) and high revisit rate of 5 days. Sentinel-2 Level-1C images were downloaded and

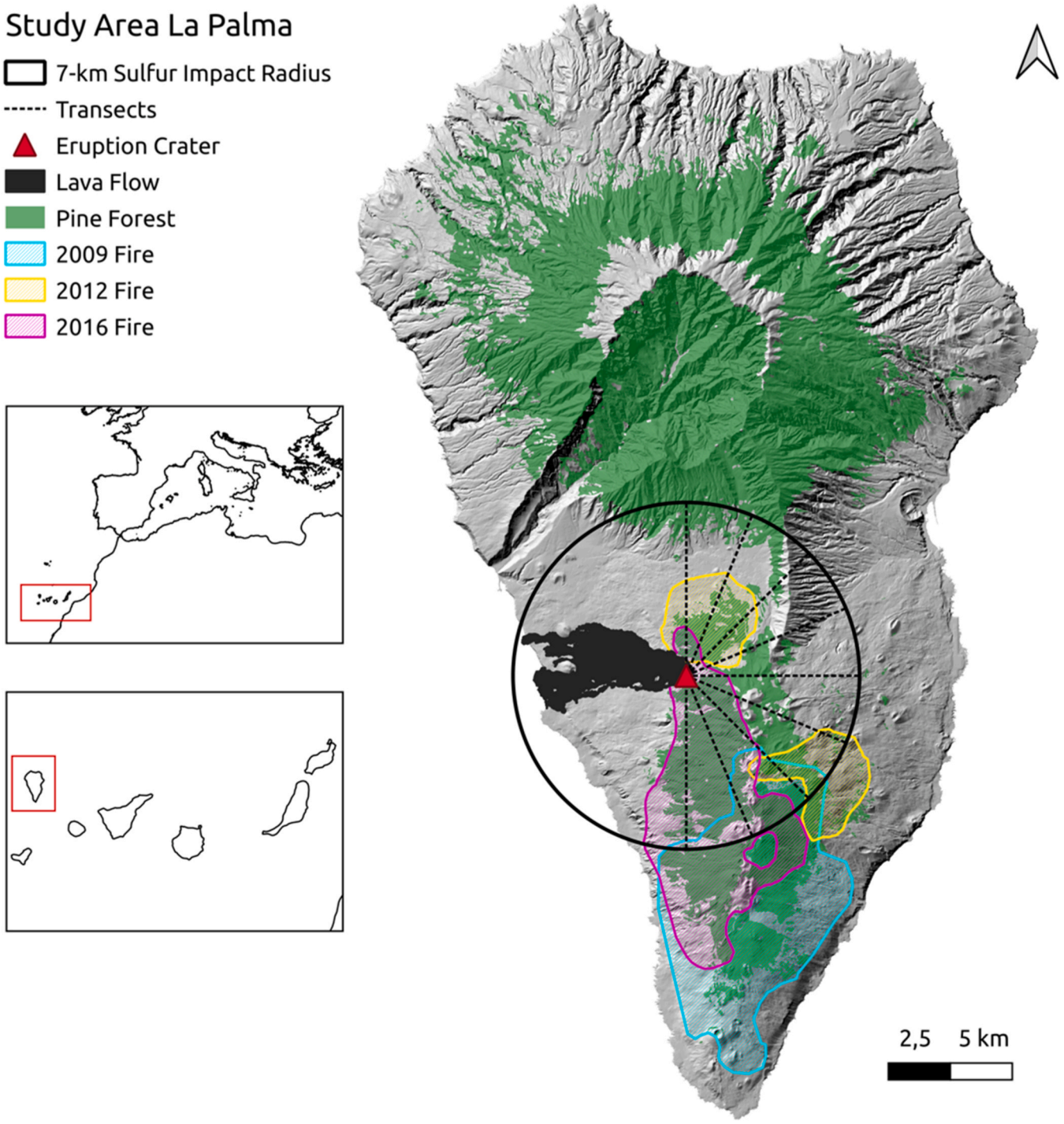

Fig. 2. Map of the study region of La Palma, Canary Islands, Spain. On the left, the inset maps illustrate the study location in relation to Europe (top box) and North Africa (bottom box). On the right, a 2 m spatial resolution DEM hillshade is presented (CNIG, 2022). The sampling design is delineated within a solid black line representing the 7 km impact radius denoted in Weiser et al. (2022) and black dashed lines represent transects in each cardinal direction. The pine forest is shown in green, and the past fires are indicated as follows: light blue = 2009 fire, yellow = 2012 fire, purple = 2016 fire. Map was created using QGIS 3.22.7-Białowieża (QGIS, 2024).

preprocessed using FORCE (Framework for Operational Radiometric Correction for Environmental Monitoring) version 3.7.10 (Frantz, 2019). FORCE is a comprehensive open-source processing engine that generates Analysis Ready Data (ARD). FORCE deploys the datacube concept, which segments images into a grid where each tile is harmonised, standardised, and radiometrically consistent while still retaining all per-pixel quality information and spectral values. FORCE ImproPhe (Improving the spatial resolution of land surface Phenology) was used to enhance the spatial resolution of Sentinel-2 20 m spectral bands to 10 m resolution. A 30 m Digital Elevation Model (DEM) from the Shuttle Rader Topography Mission (SRTM) (USGS, 2000) is used for topographic correction, enhanced shadow detection, and scaling optical depths with elevation. Only images with less than 75 % cloud cover were used.

P. canariensis forest ecosystems harbour few species in the understory. For this reason, we use the Normalised Difference Vegetation Index (NDVI) as a proxy for forest health since we can attribute most greenness to pine trees. Dense patches of understory vegetation can sometimes be encountered, e.g. shrubs such as *Cytisus proliferus* L. F. or *Lotus campylocladus* ssp. *hillebrandii* (Christ) Sandral & D.D.Sokoloff, which can cover vast patches of forest floor after wildfires, given enough precipitation (Weiser et al., 2021). However, these patches are in our experience limited to Canary Pine forest with dense canopy cover due to their need for moisture from fog precipitation, which should therefore not affect the NDVI in satellite imagery. In addition, several dry years during our study period further reduces the effect of the understory vegetation on NDVI. NDVI was generated within FORCE using the Time Series Analysis submodule (TSA). All pixel values across the study area were then interpolated at 5-day intervals across the full Sentinel-2 mission duration (Sep 2015 – March 2023). FORCE utilizes an ensemble of Radial Basis Function (RBF) convolution filters. With this method, the time series is not fitted as is commonly done with other interpolation techniques such as splines. Instead, the method deploys a moving average filter that weighs observations according to a Gaussian distribution. Since our time series has inconsistent data gaps, we used multiple kernels of different widths and aggregated their estimates using a weighted average. This allows us to make better interpolation predictions by giving preference to kernels with better data availability (Frantz, 2019). We created such a long time series to ensure that the seasonal and trend components are well established before analyzing the time series from the end of the eruption period (December 2021– March 2023).

We established transects in each cardinal direction through the remaining pine forests within a 7 km radius of the crater. Since no forest exists to the west of the crater, we only sampled pixels ranging from due north to due south in 22.5° steps for a total of nine transects (Fig. 2). We extracted time series along transects at 10 m intervals starting from the crater, this was later aggregated to the median of each 100 m interval to increase the overall robustness of the dataset by ensuring that every selected pixel is representative of the pine forest. Since several craters are close to the eruption area, we excluded all data points within 200 m from the craters from the analysis. To ensure all sampled pixels are forested, we excluded any pixels with less than 30 % tree cover density according to the Copernicus Tree Cover Product (CLMS, 2022). This yielded a dataset consisting of 476 data points, each comprising an NDVI time series.

We calculate the Theil-Sen median slope for each of the 476 extracted NDVI time series. Using the *trend* R package (Pohlert, 2023), the Theil-Sen slope (sometimes referred to the Theil-Sen estimator or Sen's slope estimator) calculates the median slope between all pairs of observations across each NDVI time series, effectively estimating a single recovery rate for each time series at each data point (Sen, 1968; Vanderhoof and Hawbaker, 2018). Using the median slope determines a reasonable estimation for the slope, or rate of recovery, in a population and is robust to outliers (Wilcox, 2001). In addition, the Theil-Sen estimator often achieves a smaller standard error than the least squares estimator and has, on average, proven to be a more accurate estimate of the true slope (Wilcox, 2001).

Forest height measurements are derived from the Global Ecosystem Dynamics Investigation (GEDI) mission which employs high-resolution lidar technology to capture detailed vertical structure data of forests, providing approximate measurements of canopy height. Canopy height may reflect local growth conditions influencing stand health such as soil moisture and fertility. Topographical variables elevation and slope are included as landscape features at pixel locations. An elevational gradient is found between the crater and the Cumbre Vieja ridgeline wherein forest density is much lower toward the ridgeline and is more affected by the local wind and precipitation regime along with greater solar radiation exposure Table 1.

Recent fire data was retrieved from the European Forest Fire Information System (EFFIS; JRC, 2018) and calculated as the number of years since the last fire. EFFIS is part of the Copernicus Emergency Management Service that provides real-time and historical fire data for European, Middle East, and North African regions. Fire metrics for the 2009,

Table 1
List of variables used in the generalized additive model (GAM). A brief description of the data is provided along with the source.

Variable	Data Description	Data Source
Recovery Rate	Theil Sen Median Slope (Sen, 1968) of each NDVI time series along each transect. Only the median of each 100 m segment along each transect was used for analysis. Calculated using the *sens.slope()* function from the trend package v1.1.6 (Pohlert, 2023).	Sentinel−2 imagery from Copernicus. Imagery and NDVI time series were preprocessed and generated with FORCE (Frantz, 2019).
Distance	Distance from the eruption crater calculated in meters. The median Recovery Rate is extracted from each 100 m segment along each transect.	and Fertility of Soils 45, 781-788. http://doi.org/10.1007/s00374-009-0389-4Points created manually using *points along geometry* function in QGIS (2024).
Direction	The direction of each sampled 7 km transect ranging from North to East to South at 22.5° intervals (e.g., 0 (North, N), 22.5 (North-Northeast, NNE), 45 (Northeast, NE), etc.).	Created manually in QGIS (2024).
Years Since Fire	Number of years since the occurrence of a fire (numeric). The last fires occurred in 2016, 2012 and 2009, respectively. However, we assumed the 2009 stands were fully recovered before the eruption and therefore we grouped these stands together with unburned stands.	European Forest Fire Information System (EFFIS; JRC, 2018).
Slope	The inclination of the terrestrial surface measured in degrees resampled at 10 m spatial resolution. Calculated based on a 2 m DEM of La Palma using the *terrain()* function in the terra package v1.7–71 (Hijmans, 2024).	Centro Nacional de Información Geográfica (2022)
Elevation	The elevation of the sampled location in meters, resampled to 10 m spatial resolution.	Centro Nacional de Información Geográfica (2022)
Forest Height	A spaceborne-based Lidar Forest height measurement from GEDI at 25 m spatial resolution resampled to 10 m to match Sentinel−2 imagery.	Global Land Analysis and Discover team at the University of Maryland (Potapov et al., 2021)
Forest Density	Forest density at 10 m spatial resolution using to filter dataset to include only pine stands with at least 30 % canopy coverage.	Copernicus Land Monitoring Service (CLMS, 2018)

2012 and 2016 fires are reported in Table 2.

A correlation analysis was performed to test for highly correlated variables within the dataset. This prevents further analysis from being subject to autocorrelation while simplifying the overall variation in the dataset. The correlation analysis was done using the *corrplot* R package (Wei and Simko, 2021), and a high correlation was found between forest density and forest height (Fig. 3). Forest density also has a small correlation with distance and was already used to filter our data to forested areas, so we removed it from the analysis. Collinearity was then checked via the variation inflation function vif() in the *usdm* package (Naimi et al., 2014) and none was found between the remaining predictors.

The final dataset was aggregated to the median value of each 100 m transect interval and is comprised of Theil-Sen median slope (hitherto referred to as recovery rate), transect direction, distance from the crater (m), elevation (m), slope (°), forest height (m) and years since last fire. Fire severity was not assessed since the level of fire intensity is confined to the amount of available fuel. Since Canary Island pine forests rely mainly on needle litter for igniting and spreading fire (Höllermann, 2000). We do not assess fire frequency or the overlap between fire events since the overlap between the 2012 and 2016 fires in minimal and *P. canariensis* canopies show little evidence of fire after 2–3 years (Molina-Terrén et al., 2016).

2.3. Statistical analyses

The recovery rate was fitted to a Generalized Additive Model (GAM) using the R package *mgcv* (Wood and Wood, 2015). GAMs are a type of regression model that allows for modelling nonlinear relationships between response and predictor variables (Wood 2017). While GAMs build on the additive structure of Generalized Linear Models (GLM), they are more suitable for multifactor analysis as linear terms of GLMs are replaced with non-parametric functions in GAMs (Hastie & Tibshirani, 2014). GAMs allow for curves when fitting the regression line to account for the complexity within the data. The amount of flexibility in the smoothing term is measured using effective degrees of freedom (EDF). EDF is constrained to the number of smoothing functions (k) for the predictor variables, with a low EDF indicating less flexibility. In comparison, a higher EDF suggests a more complex term with greater flexibility (Hastie, & Tibshirani, 1986). The model was fitted using the following formula:

$$\text{Recovery Rate} \sim s(\text{Distance, by} = \text{Direction}) + s(\text{Distance, Years Since Fire}) + s(\text{Slope}) + s(\text{Elevation}) + s(\text{Forest Height}), \text{correlation} = \text{corAR1}(\text{form} = \sim \text{Distance})$$

where s() terms refer to smoothing parameters. Here, distance from the crater (Distance) was fit a smoothing parameter in each transect direction (Direction) to assess whether certain areas may be recovering faster than others while accounting for the broad differences between distinct transect characteristics. Regarding the potential effect of fire history on recovery rate following the eruption, we fit an interaction term that includes Distance and years since the last fire (Years Since Fire). Since Distance is not modelled as a single predictor, estimating the total effect of Distance on the model is difficult. Topographic variables (Slope, Elevation) and forest height were fit using smoothing parameters. Finally, to account for spatial autocorrelation between predictors, we included an auto-regressive correlation structure in the model using the function *corAR1()* from the *mgcv* package. This was done for Distance since this is the main spatial term and Weiser et al. (2022) found forest damage to be strongly striven by stand distance to the eruption crater.

We use explained deviance to measure the goodness of model fit and use the F value, to compare the amount of explanatory power added by the smooth term of each variable. F value is commonly used as a measure of effect and a higher the F value indicates improved model fit (Wood 2017). We use the terms F value and effect size interchangeably throughout the remainder of the text. In addition, we used the *MakiCV.nlme()* function (Kiene, 2024) to perform a k-fold cross-validation (CV) to ensure model stability for making predictions. After including five folds with 100 repetitions, the CV yielded an RMSE of 1.0431 and a standard deviation of RMSE of 0.1629, indicating an adequately accurate and stable model.

Table 2
List of recent fires on La Palma according to the European Forest Fire Information System (EFFIS) product. Metrics include total area burned (ha.) and coniferous forest area burned within that total area (%). Pine forest area burned (%) reflects the proportion of coniferous forests burned within the total area burned per fire. This metric does not reflect the proportion of burned coniferous forest in relation to the entire island.

Fire Year	Total area burned (ha)	Forest area burned within each burned area (%)
2009	6073	55.3
2012	1128	54.3
2016	4629	68.7

3. Results

The GAM demonstrates high explanatory power, accounting for 88.3 % of the explained deviance across the dataset (Table 3). All the predictors were significant except for the E and ESE transects. These variables also had little impact on the recovery rate when compared to the other variables across the model, given that ESE had the lowest F value (effect size) and E had an EDF of less than one, indicating no or just a neglectable explanatory power.

The mean distance of all transects from the crater demonstrates a strong pattern with recovery rate. While pine stands within roughly 200 m of the crater still do not appear to be recovering, recovery rate then peaks around 1000 m away from the crater before gradually declining with distance (Fig. 4A, B). Distance was not modelled as a single predictor, but as an interaction term with either transect direction or years since fire. Therefore, no effect size can solely or directly represent the total effect size of distance on the model. Variables modelled with distance have F values ranging from 1.465 (Direction ESE) to 11.605 (years since fire).

The interaction between distance and years since fire was highly significant and had the greatest effect on the model with an effect size of 11.605. The stands burned by the 2016 fire had the highest median recovery rate with a Theil-Sen median slope of 4.50. This is followed by pine stands burned in 2012 (4.43), 2009 (4.14) and unburned stands (3.86) (Fig. 5A). The model reported a standard error between 0.31 and 0.33 for each fire (Fig. 5B).

Of the two topographic variables, only elevation had a significant effect on the model. Elevation had a low effect on recovery rate with an effect size of 2.736. The recovery rate appears to be highest at an elevation of about 1200 m when considering the locally estimated scatterplot smoothing (loess). However, recovery rate seems to hit its maximum anywhere from 900 – 1300 m (Fig. 6A). Slope has the second lowest effect on the model with an effect size of 1.844 and recovery rate appears highest around a slope of 27° while the maximum seems to be reached at a slope ranging from 8 to 32° (Fig. 6B).

The final predictor, forest height, had a significant effect on the model with an effect size of 8.721, the highest among predictors not modelled with distance. Recovery rate has a positive overall correlation with forest height as recovery rate increases with forest height (Fig. 7). Maximum recovery rate is reached in pine stands with a height between 12 – 18 m but appears to increase in stands 30 m tall.

4. Discussion

4.1. Distance and direction

In this study, we investigated the environmental parameters driving

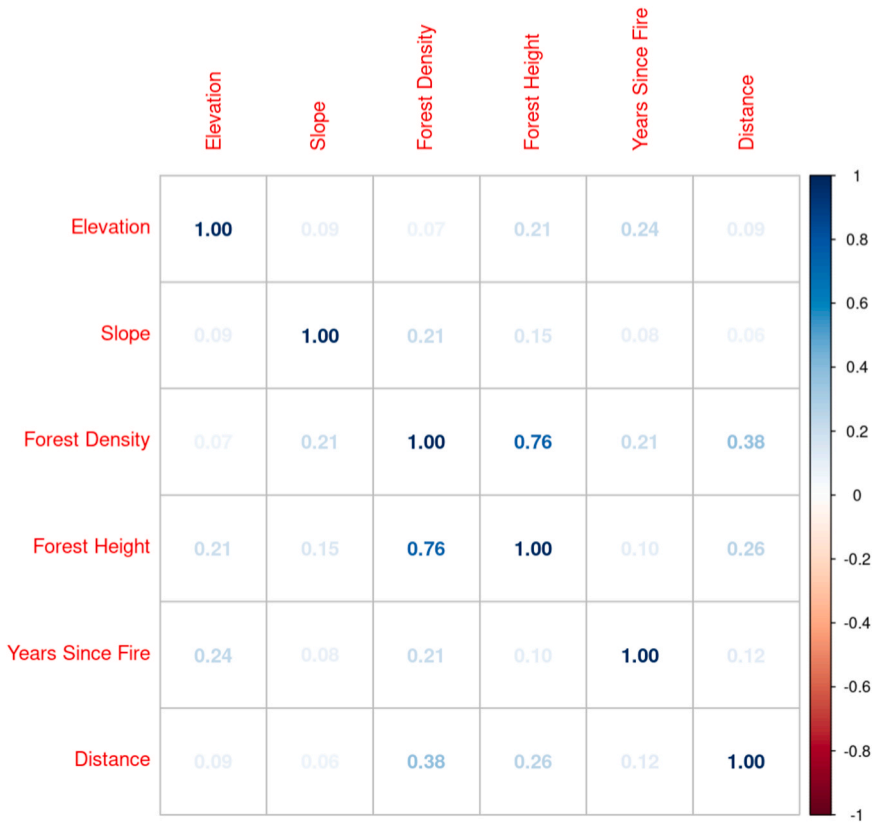

Fig. 3. Correlation analysis of predictor variables for input in the generalized additive model (GAM). Blue hues correspond to a strong positive correlation between predictors on the two axes and red hues correspond to a strong negative correlation between predictors.

Table 3
Summary of parameters used in the generalized additive model (GAM) explaining recovery rate. The recovery rate is estimated using the Theil-Sen median slope. Basis functions (k) were adjusted according to the smoothing parameters (s) of individual variables, and no additional scale parameters were used. Transect directions are denoted as follows: N = North, NNE = North-Northeast, NE = Northeast, ENE = East-Northeast, E = East, ESE = East-Southeast, SE = Southeast, SSE = South-Southeast, S = South. Effective degrees of freedom (EDF) were measured for the smoothing terms and represent the overall complexity and fit of the curve to the model. EDF values of nearly one represent a near-linear correlation while less than one show little to no effect on the response variable. The F value is a measure of the effect size the predictor has on the response variable. Deviance explained is the goodness of fit measure for the GAM.

GAM Parametric coefficients:				
	Estimate	**Std. Error**	**t-value**	**Pr(>|t|)**
(intercept)	3.93089	0.05991	65.61	<2e−16 ***
GAM Approximate significance of smooth terms:				
	EDF	**Ref.df**	**F**	**p-value**
s(Distance):DirectionN	5.476	6.213	4.872	6.77e−05 ***
s(Distance):DirectionNNE	8.455	8.775	3.772	0.000156 ***
s(Distance):DirectionNE	3.840	4.700	5.222	0.000159 ***
s(Distance):DirectionENE	8.407	8.769	4.719	8.70e−06 ***
s(Distance):DirectionE	0.900	0.900	2.730	0.117798
s(Distance):DirectionESE	3.518	4.321	1.465	0.210743
s(Distance):DirectionSE	6.647	7.679	2.123	0.032644 *
s(Distance):DirectionSSE	8.345	8.761	5.493	1.04e−06 ***
s(Distance):DirectionS	7.845	8.505	2.614	0.008831 **
s(Distance, Years Since Fire)	22.022	25.896	11.605	< 2e−16 ***
s(Slope)	2.240	2.856	1.844	0.107824
s(Elevation)	5.062	6.125	2.736	0.011708 *
s(Forest Height)	7.995	8.721	8.721	3.81e−05 ***
n=476	**Deviance Explained = 88.3 %**			

the recovery rate of *P. canariensis* stands following the 2021 Tajogaite eruption using only Earth Observation technology, demonstrating its growing utility in the field of ecology. The eruption allows for an assessment of how the Canary Island pine forest ecosystem responds to multiple, overlapping disturbances. In doing so, we contribute to the extensive body of research on the resilience of *P. canariensis* by assessing its response to a disturbance other than fire.

Distance was an impactful variable in determining the recovery rate of pine stands in our model, given the effect size of each of the transects and the interaction with recent fire history. This agrees with the results of Weiser et al. (2022), which concluded that the browning effects caused by SO_2 exposure can be observed in satellite imagery, and the magnitude of change can be estimated using NDVI. The eruption decimated pine stands in the immediate surroundings of the crater as the eruption generated massive shifts in the earth, including volcanic bombs and pressure waves that led to unstable ground and mechanical failure of trees. Thus, the trees in the close vicinity of the crater did not recover to any state of greenness, which is also supported by the data of Guerrero-Campos et al. (2024). This is in line with our first hypothesis, where the first few points within 200 m of the crater have a recovery rate of less than or nearly zero. The recovery rate peaks around 1000–1200 m away from the crater where surviving pine stands were more severely impacted by SO_2 emissions. SO_2 emissions have declined since the end of the eruption but are ongoing, with recent measurements showing an emission of 2–3 Mg per day in April 2023 (Weiser et al., 2023). Given that emissions are lower now than during the eruption, pine stands may persist through the disturbance as the intensity has decreased.

Farther away from the crater, stands have a lower recovery rate. We find that there may be a few reasons why this is. The low recovery rate of distant stands could be due to less exposure to SO_2 emissions compared to stands close to the crater. This results in a smaller difference between minimum and maximum NDVI and, subsequently, a lower Theil-Sen

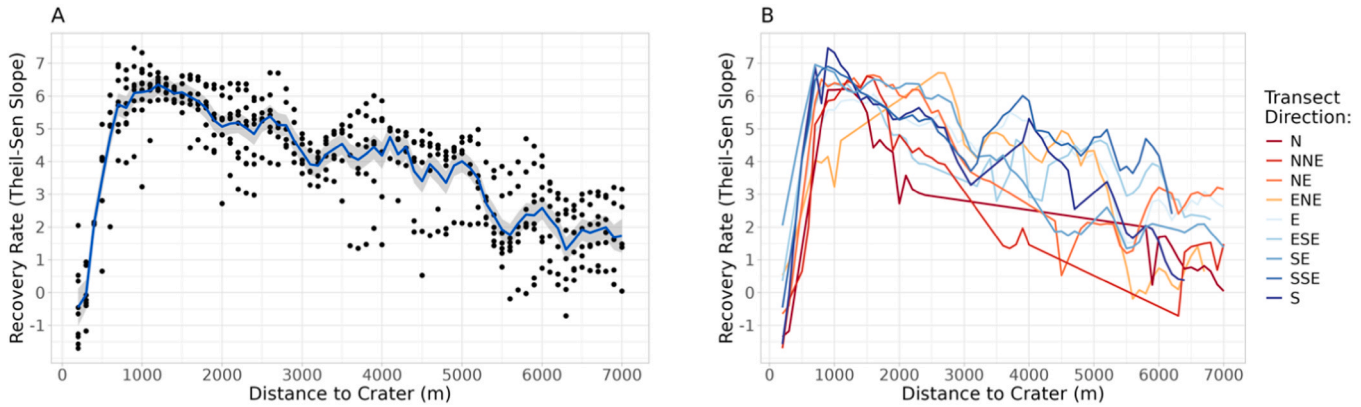

Fig. 4. The generalized additive model (GAM) shows the relationship between distance to the crater (m) and median recovery rate (A) and recovery rate for every transect (B). The recovery rate is calculated using the Theil-Sen median slope. A presents the model prediction median recovery rate of all combined transects in blue with the grey ribbon representing the 95 % confidence intervals and the residuals shown as black points. In B, the line of each transect is colored ranging from red to blue and labeled the following order: N = North, NNE = North-Northeast, NE = Northeast, ENE = East-Northeast, E = East, ESE = East-Southeast, SE = Southeast, SSE = South-Southeast, S = South. The solid lines represent the model prediction fitted to each transect.

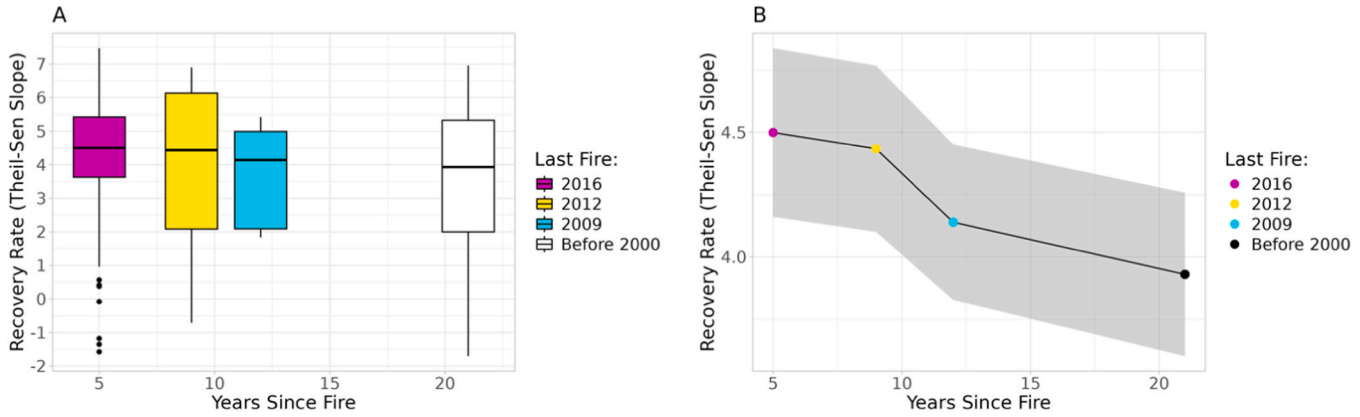

Fig. 5. The generalized additive model (GAM) shows the relationship between years since fire and recovery rate (calculated using the Theil-Sen median slope) for all points. The colored boxplots (A) and points (B) indicate the year of the last known fire in years 2016 (purple), 2012, (yellow), 2009 (light blue), or earlier than what is presented in the EFFIS dataset dating back to the year 2000 (white/black). The hinges of the boxplots represent the first and third quantiles, the whiskers present the range of values (outliers displayed as individual points), and the center line is the median (A). In plot B, the model prediction is presented as a solid black line and the 95 % confidence interval is shown as a grey ribbon.

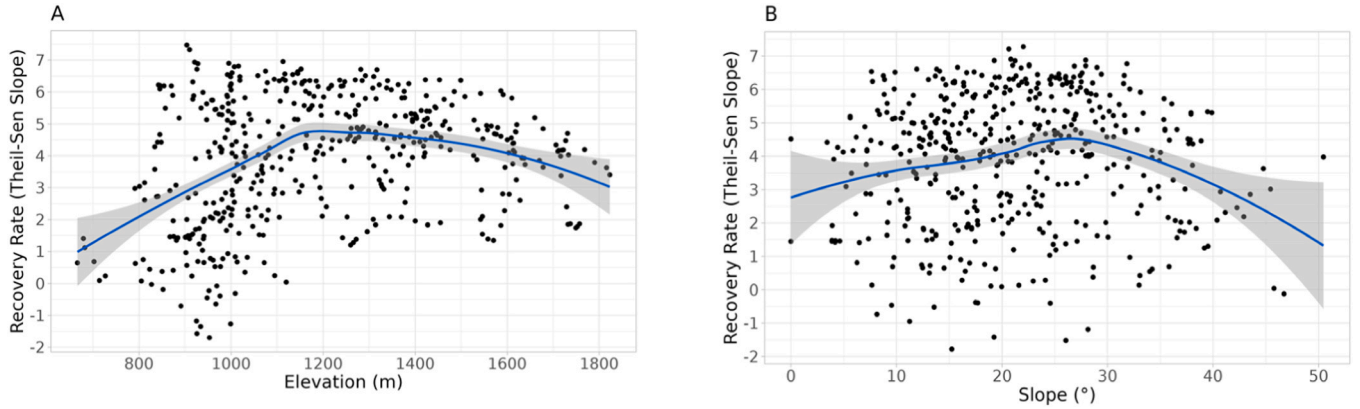

Fig. 6. The generalized additive model (GAM) shows the relationship between (A) elevation (m) and (B) slope (°) with recovery rate (calculated using the Theil-Sen median slope) for all points. The solid blue line represents the model prediction fitted using smoothing parameters. The blue line is plotted using a locally estimated scatterplot smoothing (LOESS) to display the general trend of the data. The residuals are shown as black points and 95 % confidence intervals as grey ribbons.

median slope estimate (Appendix A).

Understanding the pattern observed in the different transects is difficult without local temperature, precipitation, soil, and wind data. La Palma receives trade winds from the Northeast. Although winds were not very strong during the eruption (Milford et al., 2023), normal wind patterns may have resumed in the two years since. Wind data from the

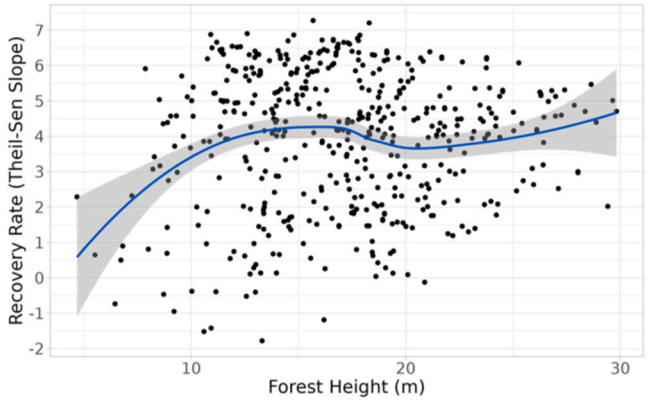

Fig. 7. The generalized additive model (GAM) shows the relationship between forest height (m) and recovery rate (calculated using the Theil-Sen median slope) for all points. The solid blue line represents the model prediction fitted using smoothing parameters. The blue line is plotted using a locally estimated scatterplot smoothing (LOESS) to display the general trend of the data. The residuals are shown as black points and 95 % confidence intervals a grey ribbon.

La Palma weather station (located 5.5 km from the crater) show that winds mostly came from the east and northeast during the eruption (Nogales et al., 2022). Weiser et al. (2022) found that forest patches south of the crater were more affected than those to the north or east, while Bonadonna et al. (2022) linked tephra distribution to wind direction since most ash and tephra deposits were found southwest and northeast of the crater. Thus, it is likely that southern transects were exposed to more SO_2 emissions, but this cannot be confirmed without data from transects west or southwest of the crater.

Incorporating local wind dynamics on the western slope of the Cumbre Vieja ridge would prove challenging as eddy covariance towers or micro weather stations would need to be situated across the entire hillside for sufficient coverage. When wind blows over a ridge, it is diverted and forms a complex lee side recirculation (Bonadonna et al., 2022). This redirects SO_2 that would otherwise disperse in the dominant wind direction, into other directions. Leeward eddies may therefore alter the deposition and distribution of airborne nutrients that influence physiological processes of plants, such as SO_2 uptake. This could explain the varying recovery rate and effect size of each transect in the model. In particular, the significance and effect size of transects in line with the dominant wind regime (NE, ENE and S) warrant consideration regarding the role of wind in redistributing SO_2 and how this may influence recovery rate. This may contradict the findings of Weiser et al. (2022) and Bonadonna et al. (2022) that highlight the role of wind in its ability to explain the distribution of needle chlorosis and tephra deposition to the south. However, we find it an essential variable to include in subsequent analyses since the recovery rate of some pine stands cannot be fully explained by the variables tested here.

4.2. Fire and disturbance interactions

Compounding disturbances of unnatural intensity or shortened return interval can lead to novel outcomes that negatively impact the resilience of an ecosystem (Turner et al., 2020). We hypothesized that stands burned by the 2016 fire would be slowest to recover from SO_2 exposure, as they were likely still in the process of recovering from the first disturbance when the eruption occurred. Here, we observe that despite facing a second disturbance in quick succession, stands affected by the 2016 wildfire are recovering faster than unburned stands (Fig. 5). The recent fires observed in this study had an uneven distribution within the dataset which limits our ability to confirm whether the recovery rate is strongly tied to recent fire history of pine stands. The standard error generated by the model, ranging from 0.31 to 0.33 for each fire, is highly variable, possibly due to insufficient temporal coverage of fire. While the effect size of the interaction between distance and years since fire is the highest in our model, we suspect that the effect of distance from the crater, which indicates exposure to volcanism, is driving this effect. This is supported by the interaction between distance and transects. Furthermore, despite having employed a correlation structure to account for the potential autocorrelation of distance, distance nonetheless displays an overwhelming effect in the model across variables.

In fire-adapted species, resilience is often supported by one of two main strategies: 1) vegetative resprouting of mature individuals or 2) massive establishment and recruitment of seedlings following a fire (Keeley & Zedler, 1998; Pausas & Keeley, 2014). Although we focus on how compounding disturbances impact resprouting, the resilience of the Canary Pine forest is also strengthened by its serotinous traits, which are known to promote the establishment of high numbers of seedlings following a wildfire (Höllermann, 2000; Otto et al., 2010; Méndez, 2010; Méndez et al., 2015). While individual mature trees may easily survive a fire due to thick bark and epicormic resprouting, the long-term perspective of the ecosystem is ultimately maintained by seedling establishment and juvenile recruitment. There is evidence that serotiny in *P. canariensis* is stimulated by the volcanic eruption, as Wilkens et al. (in review) observed massive first-year seedling establishment near the crater in early 2023. However, stands that had been affected by the 2016 wildfire showed relatively diminished establishment of one-year-old seedlings, highlighting the role of compounding disturbances in creating unpredictable effects.

4.3. Topographic factors & forest height

We included local stand characteristics of pine stands to explore the effects of other environmental variables that may influence the recovery rate of pine stands following the volcanic eruption. An optimum recovery rate is found in both elevation and slope. Recovery rates increase with elevation before declining from roughly 1200 m and higher. This decline toward the ridgeline could be due to increasing solar radiation and decreasing forest density, which combine to create a dry understory in the rain shadow of the Cumbre Vieja ridge. The ecosystem transitions into Fayal-brezal on the windward side of the ridge, indicating a precipitation regime shift from dry to moist (Irl et al., 2014). On this eastern, windward side of the Cumbre Vieja, vegetation is lush and more diverse due to the moisture brought by trade winds from the Mediterranean. Whereas on the western side of the ridge, where the new volcano has emerged, the Canary Pine dominates the dry, species-poor ecosystem. This precipitation phenomenon similarly occurs on other oceanic islands, such as the Hawaiian Islands, where the windward side of ridges are moister than their leeward counterparts (Giambelluca et al., 2011; Zhang et al., 2016).

The pattern that slope follows in the multivariate GAM is in line with the expectations set by Mora et al. (2016), as we find the recovery rate to be slightly slower on very steep slopes. On steeper slopes, fewer nutrients are available due to increased erosion and runoff (Mora et al., 2016). Most stands are located on slopes between 4° and 40° and were faster to recover than those above 40°. In addition to SO_2 emissions, ash and tephra blanketed the island with roughly 23 million m^3 of tephra deposited across the island (Bonadonna et al., 2022; Shatto et al., 2024). Though ecosystems are adapted to new tephra deposits, fresh tephra layers may divert water and nutrients in the short term, impacting the recovery of particular stands.

4.4. Forest height

To our surprise, forest height had a significant effect on our model and displayed a higher recovery rate in taller stands than in shorter stands. The height of pine stands in our model is based on lidar measurements from GEDI, which is aggregated to a spatial resolution of 25 m (Potapov et al., 2021). While the patterns observed in tall stands

could simply be attributed to local environmental parameters influencing growth conditions, tall trees are generally less susceptible to crown fire because their branches are elevated high above the forest floor (Climent et al., 2006), and thus may have been less impacted by recent fires. However, these characteristics of *P. canariensis* have yet to be understood fully in the context of volcanism, particularly intense SO_2 exposure. Trees are highly vulnerable to SO_2 damage, but their sensitivity varies significantly among species, individual trees, and different ages (Knabe 1976; Keller et al., 1997; Białobok et al., 1980; Manninen & Huttunen, 2000). This variability makes it challenging to apply findings from one species to another, or even assess the response of a single species to disturbance, without established height growth curves. Specifically, there are no existing studies on how *P. canariensis* recovers from SO_2 exposure, making it difficult to infer its sensitivity based on research on other species.

5. Conclusion

The 2021 Tajogaite eruption on La Palma provided a valuable opportunity to assess the resilience of *P. canariensis* stands to overlapping volcanic and fire disturbances. In our study, we found that the distance pine stands were from the eruption was the most critical factor influencing their recovery rate, with stands at intermediate distances from the eruption crater showing a higher recovery rate than stands farther away. In addition, recovery rate was enhanced when stands experienced a recent forest fire in 2012 or 2016, hinting at the importance of the local fire regime. While local environmental factors such as topography and stand height come into play, they are overshadowed by the impact of recent disturbances. Despite the unique ability of *P. canariensis* to resprout rapidly following disturbances, including fire and SO_2 exposure, our study underscores the need for continued monitoring of natural disturbance regimes. Our study contributes to a deeper understanding of the dynamics of Canary Pine forests and their responses to overlapping disturbances. By recognizing the role of both fire and volcanic disturbances, we can better adhere to the complex characteristics of these ecosystems and develop informed strategies for their conservation and management in the future.

CRediT authorship contribution statement

Vincent Wilkens: Data curation, Visualization, Writing – review & editing. **Tobias Heuser:** Funding acquisition, Methodology, Project administration, Writing – review & editing. **Frank Weiser:** Conceptualization, Data curation, Investigation, Methodology, Supervision, Visualization, Writing – original draft, Writing – review & editing. **Christopher Shatto:** Conceptualization, Data curation, Formal analysis, Investigation, Methodology, Software, Visualization, Writing – original draft, Writing – review & editing. **Marvin Kiene:** Conceptualization, Investigation, Methodology, Visualization, Writing – review & editing. **Peter Hofmann:** Funding acquisition, Methodology, Project administration, Resources, Writing – review & editing. **Anna Walentowitz:** Writing – original draft, Writing – review & editing.

Declaration of Competing Interest

The authors declare that they have no known competing financial interests or personal relationships that could have appeared to influence the work reported in this paper.

Data Availability

Data will be made available on request.

Acknowledgments

Funded by the KIWA project (Grant number: 67KI31043A) and the Open Access Publishing Fund of the University of Bayreuth.

We thank Carl Beierkuhnlein, Félix Manuel Medina, Manuel Nogales, María Guerrero-Campos and Patricia Marrero for their providing their expertise on this topic.

Appendix

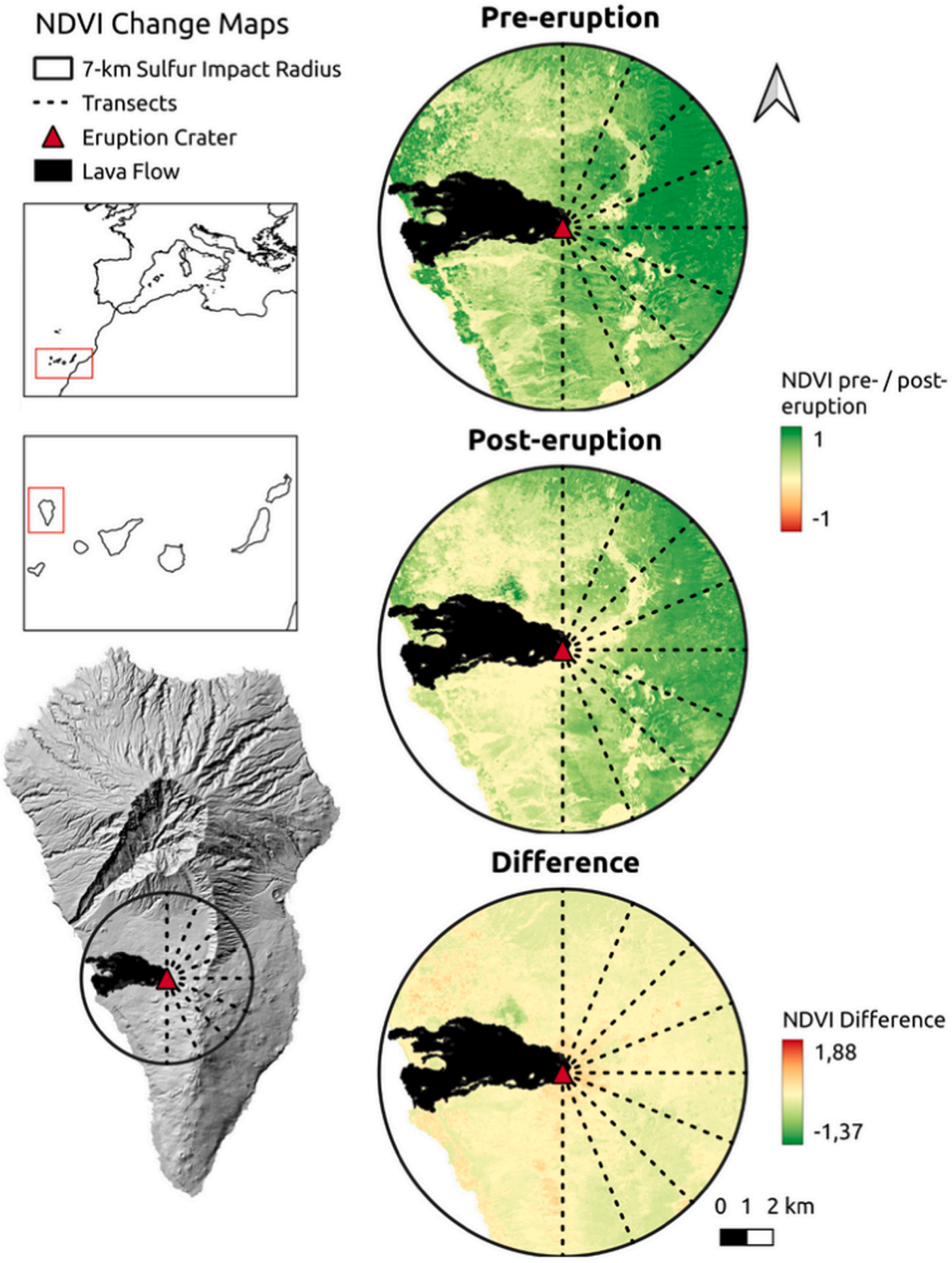

Appendix A. Map of the study region of La Palma, Canary Islands, Spain. In the left column, the inset maps illustrate the study location in relation to Europe (top), North Africa (middle), and La Palma presented with a DEM hillshade from CNIG (2022) (bottom). In the right column, 10 m maps based on cloud-free Sentinel-2 imagery display the Normalised Difference Vegetation Index (NDVI) pre-eruption on 30 Nov 2019 (top), post-eruption 14 Dec 2021 (center), and difference (bottom) within the 7-km impact radius. The pre-eruption image from 2019 is used since no cloud-free images during the same, comparable time of year were available before the eruption. The same image dates are used for NDVI change in Weiser et al. (2022). The sampling design is delineated within a solid black line representing the 7 km impact radius denoted in Weiser et al. (2022) and black dashed lines represent transects in each cardinal direction. Figure was created using QGIS 3.22.7-Białowieża (QGIS, 2024).

References

Arévalo, J.R., Fernández-Palacios, J.M., Jiménez, M.J., Gil, P., 2001. The effect of fire intensity on the understorey species composition of two Pinus canariensis reforested stands in Tenerife (Canary Islands). For. Ecol. Manag. 148, 21–29. https://doi.org/10.1016/S0378-1127(00)00478-3.

Beierkuhnlein, C., Nogales, M., Field, R., Vetaas, O.R., Walentowitz, A., Weiser, F., Stahlmann, R., Guerrero-Campos, M., Jentsch, A., Medina, F.M., Chiarucci, A., 2023. Volcanic ash deposition as a selection mechanism towards woodiness. npj Biodivers. 2, 1–8. https://doi.org/10.1038/s44185-023-00018-2.

Białobok, S., Białobok, S., Oleksyn, J., Karolewski, P., Oleksyn, J., Karolewski, P., 1980. Zmienność wrażliwości igieł drzew matecznych sosny zwyczajnej i ich potomstwa na działanie SO2, O3, mieszaniny tych gazów oraz NO2 i HF. sygn 4336, 5974.

Bonadonna, C., Pistolesi, M., Dominguez, L., Freret-Lorgeril, V., Rossi, E., Fries, A., Biass, S., Voloschina, M., Lemus, J., Romero, J., Zanon, V., Pastore, C., Reyes Hardy, M.-P., Maio, L., Gabellini, P., Martín-Lorenzo, A., Rodriguez, F., Pérez, N., 2022. Tephra sedimentation and grainsize associated with pulsatory activity: the 2021 Tajogaite eruption of Cumbre Vieja (La Palma, Canary Islands, Spain). Front. Earth Sci. 11. https://doi.org/10.3389/feart.2023.1166073.

Buma, B., 2015. Disturbance interactions: characterization, prediction, and the potential for cascading effects. art70 Ecosphere 6. https://doi.org/10.1890/ES15-00058.1.

Buma, B., Wessman, C.A., 2011. Disturbance interactions can impact resilience mechanisms of forests. Ecosphere 2, art64. https://doi.org/10.1890/ES11-00038.1.

Burton, P.J., Jentsch, A., Walker, L.R., 2020. The ecology of disturbance interactions. BioScience 70, 854–870. https://doi.org/10.1093/biosci/biaa088.

Centro Nacional de Información Geográfica (CNIG). 2022. Available online: ⟨http://centrodedescargas.cnig.es⟩ (accessed on 1 March 2023).

Chang, C.C., Halpern, C.B., Antos, J.A., Avolio, M.L., Biswas, A., Cook, J.E., del Moral, R., Fischer, D.G., Holz, A., Pabst, R.J., Swanson, M.E., Zobel, D.B., 2019. Testing conceptual models of early plant succession across a disturbance gradient. J. Ecol. 107, 517–530. https://doi.org/10.1111/1365-2745.13120.

Chano, V., Gailing, O., Collada, C., Soto, Á., 2023. Differential gene expression analysis of the resprouting process in Pinus canariensis provides new insights into a rare trait in conifers. Plant Growth Regul. 100, 717–731. https://doi.org/10.1007/s10725-023-00970-w.

1994. Clarkson, Bruce, Clarkson, Beverley, 1994. Vegetation decline following recent eruptions on White Island (Whakaari), Bay of Plenty, New Zealand. New Zealand Journal of Botany - N Z J BOT 32, 21–36. https://doi.org/10.1080/0028825X.1994.10410404.

Climent, J., Chambel, M., Pérez, E., Gil, L., Pardos, J., 2002. Relationship between heartwood radius and early radial growth, tree age, and climate in Pinus canariensis. Climent J, Chambel MR, Pérez E, Gil L, Pardos J. Can. J. For. Res. 32, 103–111. https://doi.org/10.1139/x01-178.

Climent, J., Tapias, R., Pardos, J., Gil, L., 2004. Fire adaptations in the Canary Island pine (Pinus canariensis). Plant Ecol. 171, 185–196. https://doi.org/10.1023/B:VEGE.0000029374.64778.68.

Climent, J., Chambel, M.R., López, R., Mutke, S., Alía, R., Gil, L., 2006. Population divergence for heteroblasty in the Canary Island pine (Pinus canariensis, Pinaceae). Am. J. Bot. 93, 840–848. https://doi.org/10.3732/ajb.93.6.840.

Cook, J.E., Halpern, C.B., 2018. Vegetation changes in blown-down and scorched forests 10-26 years after the eruption of Mount St. Helens, Washington, USA. Plant Ecol. 219, 957–972. https://doi.org/10.1007/s11258-018-0849-8.

Copernicus emergency management service [WWW Document] (CEMS), n.d. Copernicus EMS - Mapping. URL ⟨http://emergency.copernicus.eu/mapping/list-of-components/EMSR546⟩ (accessed 5.30.24).

Copernicus Land Monitoring Service (CLMS), 2018. Tree Cover Density 2018. ⟨https://land.copernicus.eu/pan-european/high-resolution-layers/forests/tree-cover-density/status-maps/tree-cover-density-2018⟩ (accessed on 1 March 2023).

De Nascimento, L., Willis, K.J., Fernández-Palacios, J.M., Criado, C., Whittaker, R.J., 2009. The long-term ecology of the lost forests of La Laguna, Tenerife (Canary Islands). J. Biogeogr. 36, 499–514. https://doi.org/10.1111/j.1365-2699.2008.02012.x.

Doebeli, M., Dieckmann, U., 2003. Speciation along environmental gradients. Nature 421, 259–264. https://doi.org/10.1038/nature01274.

Durán, J., Rodríguez, A., Fernández-Palacios, J., Gallardo, A., 2008. Changes in soil N and P availability in a Pinus canariensis fire chronosequence. Forest Ecology and Management. https://doi.org/10.1016/j.foreco.2008.04.033.

Durán, J., Rodríguez, A., Fernández-Palacios, J., Gallardo, A., 2009. Changes in net N mineralization rates and soil N and P pools in a pine forest wildfire chronosequence. Biol. Fertil. Soils 45, 781–788. https://doi.org/10.1007/s00374-009-0389-4.

Durán, J., Rodríguez, A., Méndez, J., Morales, G., Fernández-Palacios, J., Gallardo, A., 2019. Wildfires decrease the local-scale ecosystem spatial variability of Pinus canariensis forests during the first two decades post fire. Int. J. Wildland Fire 28. https://doi.org/10.1071/WF18145.

European Commission, Joint Research Centre (J.R.C.) (2018): Fire Database in the European Forest Fire Information System (version 2-3-1). European Commission, Joint Research Centre (JRC) [Dataset] PID: ⟨http://data.europa.eu/89h/678deb39-e35f-4236-a984-42d69bf95dec⟩.

Ernst, A., Seward, A.C., 1908. The New Flora of the Volcanic Island of Krakatau. https://doi.org/10.1017/CBO9780511703409.

Fernandes, P., Vega, J., Jiménez, E., Rigolot, E., 2008. Fire resistance of European pines. For. Ecol. Manag. 256, 246–255. https://doi.org/10.1016/j.foreco.2008.04.032.

Frantz, D., 2019. FORCE—landsat + sentinel-2 analysis ready data and beyond. Remote Sens. 11, 1124. https://doi.org/10.3390/rs11091124.

Garzón-Machado, V., Del Arco Aguilar, M., Valdés, F., Pérez-de-Paz, P., 2012. Fire as a threatening factor for endemic plants of the Canary Islands. Biodivers. Conserv. 21. https://doi.org/10.1007/s10531-012-0321-3.

Giambelluca, T., Delay, J., Nullet, M., Scholl, M., Gingerich, S., 2011. Canopy water balance of windward and leeward Hawaiian cloud forests on Haleakalā, Maui, Hawai'i. Hydrol. Process. 25, 438–447. https://doi.org/10.1002/hyp.7738.

Griggs, R.F., 2015. The Effect of the Eruption of Katmai on Land Vegetation. Bulletin of the American Geographical Society 47 (3), 193–203.

Harvey, B.J., Donato, D.C., Turner, M.G., 2016. Burn me twice, shame on who? Interactions between successive forest fires across a temperate mountain region. Ecology 97, 2272–2282. https://doi.org/10.1002/ecy.1439.

Guerrero-Campos, M., Marrero Rodríguez, P., García Becerra, R., Miranda García-Rovés, J.C., Domínguez Flores, T., Chano González, V., Fariña Trujillo, B., Nogales, M., Manuel Medina, F., 2024. Resiliencia del pinar canario después de la erupción del volcán Tajogaite (La Palma, 2021).

Hastie, T., Tibshirani, R., 1986. Generalized Additive Models.Statistical. Science 1 (3), 297–318.

Höllermann, P., 2000. The impact of fire in Canarian ecosystems 1983 - 1998. ERDKUNDE 54, 70–75. https://doi.org/10.3112/erdkunde.2000.01.06.

Hijmans, R.J., Bivand, R., Pebesma, E., Sumner, M.D., 2024. terra: Spatial Data Analysis.

IGME, 2022. Díoxido de Azufre (SO_2) en la Atmósfera. Available online: ⟨https://info.igme.es/eventos/Erupcion-volcanica-la-palma/seguimiento-erupcion⟩ (accessed on 16 April 2023).

Irl, S.D.H., Steinbauer, M.J., Messinger, J., Blume-Werry, G., Palomares-Martínez, Á., Beierkuhnlein, C., Jentsch, A., 2014. Burned and devoured-introduced herbivores, fire, and the endemic flora of the high-elevation ecosystem on la palma, Canary Islands. Arct., Antarct., Alp. Res. 46, 859–869. https://doi.org/10.1657/1938-4246-46.4.859.

Ishaq, R.M., Hairiah, K., Alfian, I., van Noordwijk, M., 2020. Natural Regeneration After Volcanic Eruptions: Resilience of the Non-legume Nitrogen-Fixing Tree Parasponia rigida. Front. For. Glob. Change 3. https://doi.org/10.3389/ffgc.2020.562303.

Johnstone, J.F., Allen, C.D., Franklin, J.F., Frelich, L.E., Harvey, B.J., Higuera, P.E., Mack, M.C., Meentemeyer, R.K., Metz, M.R., Perry, G.L., Schoennagel, T., Turner, M.G., 2016. Changing disturbance regimes, ecological memory, and forest resilience. Front. Ecol. Environ. 14, 369–378. https://doi.org/10.1002/fee.1311.

Keeley, J., 2012. Ecology and evolution of pine life histories. Ann. For. Sci. 69. https://doi.org/10.1007/s13595-012-0201-8.

Keeley, J.E., Zedler, P.H., 1998. Evolution of life histories in Pinus 219–251.

Keller, T., Rutter, A.J., Elsden, S.R., Bell, J.N.B., Hüttermann, A., Beament, J.W.L., Bradshaw, A.D., Chester, P.F., Holdgate, M.W., Sugden, T.M., Thrush, B.A., 1997. Direct effects of sulphur dioxide on trees. Philos. Trans. R. Soc. Lond. B, Biol. Sci. 305, 317–326. https://doi.org/10.1098/rstb.1984.0060.

Kent, M., Owen, N.W., Dale, P., Newnham, R., Giles, T.M., 2001. Studies of vegetation burial: a focus for biogeography and biogeomorphology. PROG. PHYS. Geogr. - PROG PHYS GEOG 25, 455–482. https://doi.org/10.1177/030913330102500401.

Kiene, M. 2024. MakiTools: an assembly of useful tools for statistics and ecology. ⟨https://raw.githubusercontent.com/Maki-science/MakiTools/main/customFunctionsMaki.R⟩.

Knabe, W., 1976. Effects of Sulfur Dioxide on Terrestrial Vegetation. Ambio 5, 213–218.

Longpré, M.-A., Felpeto, A., 2021. Historical volcanism in the Canary Islands; part 1: a review of precursory and eruptive activity, eruption parameter estimates, and implications for hazard assessment. J. Volcanol. Geotherm. Res. 419, 107363. https://doi.org/10.1016/j.jvolgeores.2021.107363.

López de Heredia, U., López, R., Collada, C., Emerson, B.C., Gil, L., 2014. Signatures of volcanism and aridity in the evolution of an insular pine (Pinus canariensis Chr. Sm. Ex DC in Buch). Heredity 113, 240–249. https://doi.org/10.1038/hdy.2014.22.

López De Heredia, U., Venturas, M., López, R.A., Gil, L., 2010. High biogeographical and evolutionary value of Canary Island pine populations out of the elevational pine belt: the case of a relict coastal population. J. Biogeogr. 37, 2371–2383. https://doi.org/10.1111/j.1365-2699.2010.02367.x.

Mack, R.N., 1981. Initial effects of ashfall from mount st. helens on vegetation in eastern washington and adjacent idaho. Science 213, 537–539. https://doi.org/10.1126/science.213.4507.537.

Manninen, S., Huttunen, S., 2000. Response of needle sulphur and nitrogen concentrations of Scots pine versus Norway spruce to SO_2 and NO2. Environ. Pollut. 107, 421–436. https://doi.org/10.1016/S0269-7491(99)00158-X.

Méndez, J., 2010. Análisis del impacto del fuego en la regeneración sexual del pino canario a lo largo de una cronosecuencia de incendios en la isla de La Palma (Canarias). Universidad de La Laguna, Canary Islands, Spain.

Méndez, J., Morales, G., de Nascimento, L., Otto, R., Gallardo, A., Fernández-Palacios, J. M., 2015. Understanding long-term post-fire regeneration of a fire-resistant pine species. Ann. For. Sci. 72, 609–619. https://doi.org/10.1007/s13595-015-0482-9.

Milford, C., Torres, C., Vilches, J., Gossman, A.-K., Weis, F., Suárez-Molina, D., García, O. E., Prats, N., Barreto, Á., García, R.D., Bustos, J.J., Marrero, C.L., Ramos, R., Chinea, N., Boulesteix, T., Taquet, N., Rodríguez, S., López-Darias, J., Sicard, M., Córdoba-Jabonero, C., Cuevas, E., 2023. Impact of the 2021 La Palma volcanic eruption on air quality: Insights from a multidisciplinary approach. Sci. Total Environ. 869, 161652. https://doi.org/10.1016/j.scitotenv.2023.161652.

Molina-Terrén, D.M., Fry, D.L., Grillo, F.F., Cardil, A., Stephens, S.L., 2016. Fire history and management of Pinuscanariensis forests on the western Canary Islands Archipelago, Spain. For. Ecol. Manag. 382, 184–192. https://doi.org/10.1016/j.foreco.2016.10.007.

Mora, J., Armas-Herrera, C., Guerra, J., Arbelo, C., Rodríguez Rodríguez, A., Notario, J., 2016. A comparative study of long-term effects on fire-affected volcanic soils in two different ecosystems in the Canary Islands. Land Degrad. Dev. 27, 1489–1500. https://doi.org/10.1002/ldr.2458.

del Moral, R., 2000. Succession and local species turnover on Mount St. Helens, Washington. Acta Phytogeogr. Suec. 85, 51–60.
del Moral, R., Grishin, S., 1999. Volcanic Disturbances and Ecosystem Recovery. : Ecosyst. Disturb. Ground 137–160.
del Moral, R., Wood, D.M., 2012. Vegetation development on permanently established grids, Mount St. Helens (1986-2010). Ecology 93, 2125.
Naimi, B., Hamm, N.A.S., Groen, T.A., Skidmore, A.K., Toxopeus, A.G., 2014. Where is positional uncertainty a problem for species distribution modelling? Ecography 37, 191–203. https://doi.org/10.1111/j.1600-0587.2013.00205.x.
Nogales, M., Guerrero-Campos, M., Boulesteix, T., Taquet, N., Beierkuhnlein, C., Campion, R., Fajardo, S., Zurita, N., Arechavaleta, M., García, R., Weiser, F., Medina, F., 2022. The fate of terrestrial biodiversity during an oceanic island volcanic eruption. Sci. Rep. 12. https://doi.org/10.1038/s41598-022-22863-0.
Nogué, S., de Nascimento, L., Fernández-Palacios, J.M., Whittaker, R.J., Willis, K.J., 2013. The ancient forests of La Gomera, Canary Islands, and their sensitivity to environmental change. J. Ecol. 101, 368–377. https://doi.org/10.1111/1365-2745.12051.
Ogle, K., Barber, J.J., Barron-Gafford, G.A., Bentley, L.P., Young, J.M., Huxman, T.E., Loik, M.E., Tissue, D.T., 2015. Quantifying ecological memory in plant and ecosystem processes. Ecol. Lett. 18, 221–235. https://doi.org/10.1111/ele.12399.
Otto, R., García-del-Rey, E., Gil Muñoz, P., Fernández-Palacios, J.M., 2010. The effect of fire severity on first-year seedling establishment in a Pinus canariensis forest on Tenerife, Canary Islands. Eur. J. Res 129, 499–508. https://doi.org/10.1007/s10342-009-0347-6.
Paine, R.T., Tegner, M.J., Johnson, E.A., 1998. Compounded perturbations yield ecological surprises. Ecosystems 1, 535–545. https://doi.org/10.1007/s100219900049.
Pausas, J.G., Keeley, J.E., 2014. Evolutionary ecology of resprouting and seeding in fire-prone ecosystems. N. Phytol. 204, 55–65. https://doi.org/10.1111/nph.12921.
Pausas, J.G., Keeley, J.E., 2017. Epicormic resprouting in fire-prone ecosystems. Trends Plant Sci. 22, 1008–1015. https://doi.org/10.1016/j.tplants.2017.08.010.
Pickett, S.T., White, P.S. (Eds.), 1985. The ecology of natural disturbance and patch dynamics. Academic Press, Orlando, Fla.
Potapov, P., Li, X., Hernandez-Serna, A., Tyukavina, A., Hansen, M.C., Kommareddy, A., Pickens, A., Turubanova, S., Tang, H., Silva, C.E., Armston, J., Dubayah, R., Blair, J. B., Hofton, M., 2021. Mapping global forest canopy height through integration of GEDI and Landsat data. Remote Sens. Environ. 253, 112165. https://doi.org/10.1016/j.rse.2020.112165.
Pohlert, T., 2023. Non-Parametric Trend Tests and Change-Point Detection.
QGIS, 2024. QGIS Geographic Information System. QGIS Association. ⟨http://www.qgis.org⟩.
Rodríguez Martín, J.A., Nanos, N., Miranda, J.C., Carbonell, G., Gil, L., 2013. Volcanic mercury in Pinus canariensis. Naturwissenschaften 100, 739–747. https://doi.org/10.1007/s00114-013-1070-1.
Sáenz-Ceja, J.E., Sáenz-Ceja, B.L., Sáenz-Reyes, J.T., Pérez-Salicrup, D.R., 2022. Conifer establishment after the eruption of the Paricutin volcano in central Mexico. For. Ecosyst. 9, 100007. https://doi.org/10.1016/j.fecs.2022.100007.
Sen, P.K., 1968. Estimates of the regression coefficient based on Kendall's Tau. J. Am. Stat. Assoc. 63, 1379–1389. https://doi.org/10.1080/01621459.1968.10480934.
Shatto, C., Weiser, F., Walentowitz, A., Stahlmann, R., Shrestha, S., Guerrero-Campos, M., Medina, F.M., Nogales, M., Jentsch, A., Beierkuhnlein, C., 2024. Volcanic tephra deposition dataset based on interpolated field measurements following the 2021 Tajogaite Eruption on La Palma, Canary Islands, Spain. Data Brief. 52, 109949. https://doi.org/10.1016/j.dib.2023.109949.
Tortini, R., van Manen, S.M., Parkes, B.R.B., Carn, S.A., 2017. The impact of persistent volcanic degassing on vegetation: a case study at Turrialba volcano, Costa Rica. Int. J. Appl. Earth Obs. Geoinf. 59, 92–103. https://doi.org/10.1016/j.jag.2017.03.002.
Tsuyuzaki, S., 1991. Species turnover and diversity during early stages of vegetation recovery on the volcano Usu, northern Japan. J. Veg. Sci. 2, 301–306. https://doi.org/10.2307/3235920.
Turner, M.G., Calder, W.J., Cumming, G.S., Hughes, T.P., Jentsch, A., LaDeau, S.L., Lenton, T.M., Shuman, B.N., Turetsky, M.R., Ratajczak, Z., Williams, J.W., Williams, A.P., Carpenter, S.R., 2020. Climate change, ecosystems and abrupt change: science priorities. Philos. Trans. R. Soc. B: Biol. Sci. 375, 20190105. https://doi.org/10.1098/rstb.2019.0105.
USGS, 2000. EarthExplorer. Retrieved March 17, 2023, from https://doi.org/10.5066/F7PR7TFT.
Vanderhoof, M., Hawbaker, T., 2018. It matters when you measure it: Using snow-cover Normalised Difference Vegetation Index (NDVI) to isolate post-fire conifer regeneration. Int. J. Wildland Fire 27. https://doi.org/10.1071/WF18075.
Veblen, T.T., Ashton, D.H., Schlegel, F.M., Veblen, A.T., 1977. Plant Succession in a Timberline Depressed by Vulcanism in South-Central Chile. J. Biogeogr. 4, 275–294. https://doi.org/10.2307/3038061.
Wei, T., & Simko, V., 2021. R package 'corrplot': Visualization of a Correlation Matrix (Version 0.92) [Computer software]. Retrieved from ⟨https://github.com/taiyun/corrplot⟩.
Weiser, F., Sauer, A., Gettueva, D., Field, R., Irl, S.D., Vetaas, O., Beierkuhnlein, C., 2021. Impacts of forest fire on understory species diversity in Canary pine ecosystems on the island of La Palma. Forests 12, 1638. https://doi.org/10.3390/f12121638.
Weiser, F., Baumann, E., Jentsch, A., Medina, F., Lu, M., Nogales, M., Beierkuhnlein, C., 2022. Impact of volcanic sulfur emissions on the pine forest of La Palma, Spain. Forests 13, 299. https://doi.org/10.3390/f13020299.
Weiser, F., Walentowitz, A., Baumann, E., Shatto, C., Guerrero-Campos, M., Jentsch, A., Nogales, M., Medina, F., Vetaas, O., Beierkuhnlein, C., 2023. Combining in-situ monitoring and remote sensing to detect spatial patterns of volcanic sulphur impact on pine needles. For. Ecol. Manag. 549. https://doi.org/10.1016/j.foreco.2023.121468.
Wilcox, R.R., 2001. Fundamentals of Modern Statistical Methods. Springer. ISBN 0-387-95157-1. ASTIN Bull. 32, 199–200. https://doi.org/10.1017/S0515036100013027.
Wilkens, V., Shatto, C., Walentowitz, A., Weiser, F., Vetaas, O.R., Medina, F., Otto, R., Guerrero-Campos, M., Nogales, M., Jentsch, A., & Beierkuhnlein, C. Wildfires and volcanic eruptions as interacting drivers of Canary pine forest regeneration. Manuscript in review.
Wood, S., & Wood, M.S., 2015. Package 'mgcv'. R package version 1.8-41, 1(29), 729.
Wood, S.N., 2017a. Generalized Additive Models: An Introduction with R, Second Edition, 2nd ed. Chapman and Hall/CRC, New York. https://doi.org/10.1201/9781315370279.
Yang, L.H., Naeem, S., 2008. The ecology of resource pulses. Ecology 89, 619–620. https://doi.org/10.1890/07-1431.1.
Zhang, C., Wang, Y., Hamilton, K., Lauer, A., 2016. Dynamical downscaling of the climate for the Hawaiian Islands. Part II: projection for the late twenty-first century. J. Clim. 29, 8333–8354. https://doi.org/10.1175/JCLI-D-16-0038.1.
Zobel, D., Antos, J., Fischer, D., 2022. Community development by forest understory plants after prolonged burial by tephra. Plant Ecol. 223, 1–16. https://doi.org/10.1007/s11258-021-01216-3.
Zobel, D.B., Antos, J.A., 1997. A decade of recovery of understory vegetation buried by volcanic tephra from mount st. helens. Ecol. Monogr. 67, 317–344. https://doi.org/10.1890/0012-9615(1997)067[0317:ADOROU]2.0.CO;2.